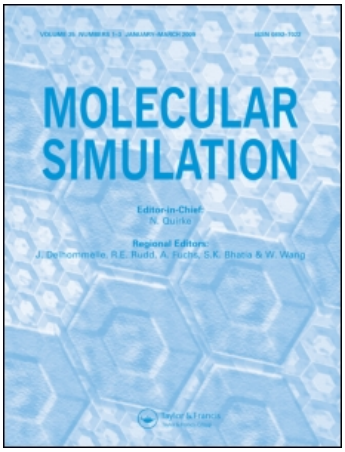

Molecular Simulation
Publication details, including instructions for authors and subscription information:
http://www.informaworld.com/smpp/title~content=t713644482

Space and Time Correlations in 2:1 and 2:2 Electrolyte Solutions

Léo Degrève[a]
[a] Faculdade de Filosofia, Ciĕncias e Letras de Ribeirão Preto, Universidade de São Paulo, Ribeirão Preto, S.P., Brazil

To cite this Article Degrève, Léo(1993) 'Space and Time Correlations in 2:1 and 2:2 Electrolyte Solutions', Molecular Simulation, 9: 6, 425 — 445
To link to this Article: DOI: 10.1080/08927029308048272
URL: http://dx.doi.org/10.1080/08927029308048272

Molecular Simulation, 1993, Vol. 9(6), pp. 425–445
Reprints available directly from the publisher
Photocopying permitted by license only

SPACE AND TIME CORRELATIONS IN 2:1 AND 2:2 ELECTROLYTE SOLUTIONS

LÉO DEGRÈVE

Faculdade de Filosofia, Ciências e Letras de Ribeirão Preto,
Universidade de São Paulo,
14049 Ribeirão Preto S.P., Brazil

(Received May 1992, accepted June 1992)

The temporal behavior of the space correlations between ions in aqueous electrolyte solutions was analysed by Brownian dynamics simulations that have produced the frequency distributions of the retention times of the ions inside definite interionic distances. The concentration range of the 2:2 and 2:1 electrolyte solutions was 0.1 to 1.0 M and the temperature fixed at 300 K. Various models were used to describe the interionic and the solute-solvent interactions. The distribution of the retention times is related to the loss of temporal correlations between the relative velocities of the ions and between the systematic interionic forces acting upon them. The decay of the frequency of the retention times is associated to an hydrodynamic decay of the correlation between the ionic velocities and to a solute-solvent process for the forces. No evidence of stable ionic pairing was obtained.

KEY WORDS: Brownian dynamics simulations, electrolyte solutions, space correlations, time correlations.

INTRODUCTION

The main objective of this paper is to present an extension to 1:2 and 2:2 electrolytes of the dynamical results obtained previously on 1:1 aqueous electrolyte solutions [1]. It will be shown that the analysis of the interionic spatial correlation functions allows access to the fundamental processes of the global interactions acting on the ions in dispersive media. Most of the equilibrium and transport properties of the electrolyte solutions must be explained by taking account of the loss of ionic translational degrees of freedom [2, 3]. The cause is the action of the dispersive, random and systematic forces, which allows the ions to approach one another until the distance where the net interaction forces are attractive forces and/or where their separation becomes difficult. No new chemical species appears [4] and the lifetime of these entities, sometimes called clusters, is short [1, 5, 6, 7]. The lifetime of local structures is also used to describe transport properties in liquid electrolytes [8].

The loss of the translational degrees of freedom modifies the number of free charges because they are transformed in internal degrees of freedom [9]. The strong deviations from ideality attributable to the electrostatic forces are also weakened [10]. Even in the so-called strong electrolyte solutions the fraction of associated ions is large, even at moderate concentrations [3, 7, 9, 11, 12]. Properties such as molar conductance depend mainly upon the fraction of free ions

and consequently upon the fraction of ions that recover quickly the translational degrees of freedom [8]. The analysis of the ionic trajectories results in a differentiation between short and long mean time behaviors [1, 4]. The corresponding equilibrium property is the ionic association that assumes its meaning when the observation is made over a long time [4]. An oppositely point of view is the determination of the loss of translational degrees of freedom on a purely dynamical basis [1, 7, 8, 13].

In this paper, the correlations between the trajectories of the ions in 2:1 and 2:2 electrolytes solutions will be investigated from the point of view of the time-dependent properties. The electrolyte solutions will be modeled by the electrolyte concentration, the short-range forces and the viscosity of the media. The features of the model are: the ions interact directly with solvent molecules and with other ions. The interionic short range interaction potential will be described by the Lennard-Jones potential because this potential handles properly the short range repulsive and attractive interactions that are important for the details of the retention times distribution. This potential is quite different from the one used in reference 12 where the r^{-9} non-Coulombic potential is repulsive. The interactions also can be indirect when occurring by means of other molecules and ions. Nevertheless, the complexity of the resulting interaction forces can be formally reduced by the introduction of the medium permittivity, the medium viscosity and random forces as registered in the Langevin equation. In this way, the Langevin equation is the basis of a model to simulate electrolyte solutions where the existence of viscous forces implicates also the Brownian collision. The resulting Brownian dynamics technique allows to access the dynamical and equilibrium properties [7, 14].

METHOD

The 2:1 and 2:2 electrolytes solutions are constituted by 108 spherical ions with a diameter, σ, equal to 0.425 nm, a mass of 0.040 kg mol^{-1} and a charge at their centres. In aqueous solutions, at $T = 300$ K, these ions experience a friction coefficient, ξ, equal to 1.03×10^{14} s^{-1}: this value and its half were used to describe the action of the viscous and random forces in the solutions. The concentration range of the electrolyte solutions was fixed between 0.1 M and 1.0 M at 300 K. The interionic interaction potential is the sum of the Lennard-Jones short-range potential with a force constant, ϵ (depth of the well), numerically equal to 150 or 300 k (k is the Boltzmann's constant) and the Coulombic potential. The permittivity of the medium is 78.5. The anions are doubly charged in the 2:1 electrolyte solutions. The electrolyte solutions were simulated by a standard algorithm for Brownian dynamics [14] using the minimum image conditions. This technique can be used because the systems are sufficiently diluted to permit to disregard a more sophisticate treatment of the long range forces [15, 16, 17, 18]. The equilibration was obtained after 3.0, 8.0 or 13.0×10^{-10} s, being the time step fixed at 5.0×10^{-15} s in all cases. The correlation functions and also the self-diffusion coefficients were calculated during 100 000 time steps. The retention times of the ions into definite interionic distances were registered in order to obtain the space correlation functions. These correlations functions were also investigated as functions of the distance from the central ion.

THEORY

The retention time distribution function for the ions i and j for interionic distances less than some R is equal, thanks to the ergodic theorem, to the time probability function for the ion j in a sphere with radius R around the central ion j:

$$P_{ij}(t+t', R) = \begin{cases} \dfrac{\langle \Delta\mathbf{r}_{ij}(t+t') \cdot \Delta\mathbf{r}_{ij}(t') \rangle}{\langle \Delta\mathbf{r}_{ij}(t') \cdot \Delta\mathbf{r}_{ij}(t') \rangle} & \text{If } |\Delta\mathbf{r}_{ij}| \leqslant R \\ 0 & \text{otherwise} \end{cases} \tag{1}$$

where $\Delta\mathbf{r}_{ij}(t')$ is the vector distance between the ions i and j at time t' when they enter into the sphere where the correlation is observed and $\langle \ldots \rangle$ an ensemble average. In this case $\Delta\mathbf{r}_{ij}(t')^2 = R^2$.

The coordinate of an ion at time $t+t'+dt$ (dt: time step) is, using the Brownian dynamics algorithm[14]:

$$\mathbf{r}_i(t+t'+dt) = \mathbf{r}_i(t+t') + \mathbf{Y}_{v,i}(t+t') + \mathbf{Y}_{s,i}(t+t') + \mathbf{Y}_{r,i}(t+t') \tag{2}$$

where $\mathbf{Y}_{v,i}(t+t')$, $\mathbf{Y}_{s,i}(t+t')$ and $\mathbf{Y}_{r,i}(t+t')$ are contributions of the velocity, the systematic and random forces successively[14]. Using the definition $\Delta\mathbf{Y}_{v,ij}(t+t') = \mathbf{Y}_{v,i}(t+t') - \mathbf{Y}_{v,j}(t+t')$, the substitution of equation (2) in (1) results in:

$$\begin{aligned} P_{ij}(t+t', R) = \frac{1}{R^2} \cdot \langle & \Delta\mathbf{r}_{ij}(t+t') \cdot \Delta\mathbf{r}_{ij}(t') + \Delta\mathbf{Y}_{v,ij}(t+t') \cdot \Delta\mathbf{Y}_{v,ij}(t') + \\ & \Delta\mathbf{Y}_{s,ij}(t+t') \cdot \Delta\mathbf{Y}_{s,ij}(t') + \Delta\mathbf{Y}_{r,ij}(t+t') \cdot \Delta\mathbf{Y}_{r,ij}(t') + \\ & \Delta\mathbf{r}_{ij}(t+t') \cdot \Delta\mathbf{Y}_{v,ij}(t') + \Delta\mathbf{Y}_{v,ij}(t+t') \cdot \Delta\mathbf{r}_{ij}(t') + \\ & \Delta\mathbf{r}_{ij}(t+t') \cdot \Delta\mathbf{Y}_{s,ij}(t') + \Delta\mathbf{Y}_{s,ij}(t+t') \cdot \Delta\mathbf{r}_{ij}(t') + \\ & \Delta\mathbf{r}_{ij}(t+t') \cdot \Delta\mathbf{Y}_{r,ij}(t') + \Delta\mathbf{Y}_{r,ij}(t+t') \cdot \Delta\mathbf{r}_{ij}(t') + \\ & \Delta\mathbf{Y}_{v,ij}(t+t') \cdot \Delta\mathbf{Y}_{s,ij}(t') + \Delta\mathbf{Y}_{s,ij}(t+t') \cdot \Delta\mathbf{Y}_{v,ij}(t') + \\ & \Delta\mathbf{Y}_{v,ij}(t+t') \cdot \Delta\mathbf{Y}_{r,ij}(t') + \Delta\mathbf{Y}_{r,ij}(t+t') \cdot \Delta\mathbf{Y}_{v,ij}(t') + \\ & \Delta\mathbf{Y}_{s,ij}(t+t') \cdot \Delta\mathbf{Y}_{r,ij}(t') + \Delta\mathbf{Y}_{r,ij}(t+t') \cdot \Delta\mathbf{Y}_{s,ij}(t') \rangle \end{aligned} \tag{3}$$

As a consequence, the correlation function $P(t, R)$ accumulates all the loss of correlation between the relative positions, velocities and systematic forces from the initial time s, and to the time $t+t'$. The ensemble averages put to zero all the non-systematic terms:

$$\begin{aligned} P_{ij}(t+t', R) = \frac{1}{R^2} \cdot \langle & \Delta\mathbf{r}_{ij}(t+t') \cdot \Delta\mathbf{r}_{ij}(t') + \\ & \Delta\mathbf{Y}_{v,ij}(t+t') \cdot \Delta\mathbf{Y}_{v,ij}(t') + \Delta\mathbf{Y}_{s,ij}(t+t') \cdot \Delta\mathbf{Y}_{s,ij}(t') + \\ & \Delta\mathbf{r}_{ij}(t+t') \cdot \Delta\mathbf{Y}_{v,ij}(t') + \Delta\mathbf{Y}_{v,ij}(t+t') \cdot \Delta\mathbf{r}_{ij}(t') + \\ & \Delta\mathbf{r}_{ij}(t+t') \cdot \Delta\mathbf{Y}_{s,ij}(t') + \Delta\mathbf{Y}_{s,ij}(t+t') \cdot \Delta\mathbf{r}_{ij}(t') + \\ & \Delta\mathbf{Y}_{v,ij}(t+t') \cdot \Delta\mathbf{Y}_{s,ij}(t') + \Delta\mathbf{Y}_{s,ij}(t+t') \cdot \Delta\mathbf{Y}_{v,ij}(t') \rangle \end{aligned} \tag{4}$$

The averages of the terms depending only on the coordinates can be obtained by using the equilibrium radial distribution functions. For example, with the introduction of the relative coordinates, the explicit expression for $\Delta\mathbf{F}_{v,ij}(t)$[14] and the velocity time dependence obtained in a stochastic model[19], we have:

$$\langle \Delta\mathbf{r}_{ij}(t+t') \cdot \Delta\mathbf{Y}_{v,ij}(t') \rangle = \langle \Delta\mathbf{Y}_{v,ij}(t+t') \cdot \Delta\mathbf{r}_{ij}(t') \rangle =$$

$$\left\langle \Delta\mathbf{r}(t') \cdot \Delta\mathbf{v}(t') \cdot \frac{1}{\xi} \cdot [1 - \exp(-\xi dt)] \right\rangle =$$

$$8\sqrt{2}\pi^2 R \frac{d-1}{d} \cdot V \cdot [1 - \exp(-\xi dt)] \cdot \left[\left(\frac{\xi}{6\pi\sigma} + D \right) t \right]^{-(d/2)} \tag{5}$$

where V is the mean velocity of the ions, D the diffusion coefficient of the solute molecules and d the dimensionality of the system and t' some time. The most important feature of equation (5) is its time, $t^{-(d/2)}$ relationship.

Another important term in equation (4) is obtained introducing the systematic forces dependence[14]:

$$\langle \Delta\mathbf{r}_{ij}(t+t') \cdot \Delta\mathbf{Y}_{s,ij}(t') \rangle = \langle \Delta\mathbf{Y}_{s,ij}(t+t') \cdot \Delta\mathbf{r}_{ij}(t') \rangle =$$

$$\left\langle \Delta\mathbf{r}(t') \cdot \Delta\mathbf{f}(t') \cdot \frac{[\xi dt - 1 + \exp(-\xi dt)]}{m\xi^2} + \right.$$

$$\left. \Delta\mathbf{r}(t') \cdot \Delta\mathbf{f}'(t') \cdot \frac{[\frac{1}{2} \cdot (\xi dt)^2 - \xi dt + 1 - \exp(-\xi dt)]}{m\xi^3} \right\rangle =$$

$$H(t+t') \cdot 4\pi R \cdot \int_0^R g_{ij}(r) \cdot \exp(-\beta\{E_{Cou} + E_{LJ}\}) \cdot r^2 dr \cdot$$

$$\left[f(r) \cdot \frac{[\xi dt - 1 + \exp(-\xi dt)]}{m\xi^2} + f'(r) \cdot \frac{[\frac{1}{2} \cdot (\xi dt)^2 - \xi dt + 1 - \exp(-\xi dt)]}{m\xi^3} \right] \cdot$$

$$\frac{1}{\int_0^R g_{ij}(r) \exp(-\beta\{V_{Cou} + V_{LJ}\} r^2 dr} \tag{6}$$

where V_{Cou} and V_{LJ} are the Coulomb and Lennard-Jones potentials successively, $\mathbf{f}$ and $\mathbf{f}'$ the systematic force and its first derivative, $H(t+t')$ a function describing the decay of the correlations during the time interval t' to $t+t'$, $g_{ij}(r)$ is the radial distribution function for the i and j ions and $\beta = (kT)^{-1}$.

RESULTS AND DISCUSSION

In order to be sure that the model potentials are realistic enough so that the results may be applied to real solutions, one transport property was first determined for the systems to be studied. The self-diffusion coefficients are plotted in Figure 1. The standard deviations were found to be in the range 6 to 7% for the systems where $\xi = 0.52 \cdot 10^{14}\,s^{-1}$ while they are a little smaller (4 to 6%) in the cases where $\xi = 1.03 \cdot 10^{14}\,s^{-1}$. The errors do not depend on the concentrations. The interaction potential used here introduced the most important facts on the short (attraction and repulsion) and long range interactions in the same way than a more

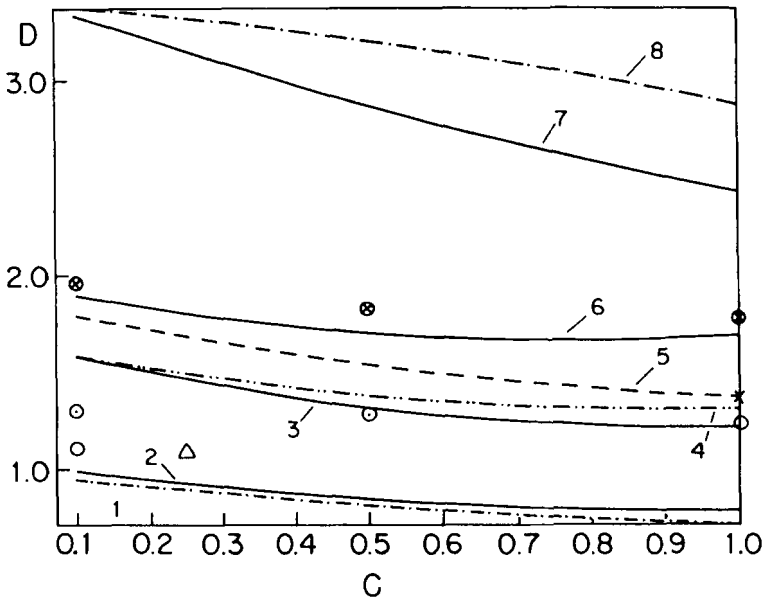

Figure 1 The self-diffusion coefficient as a function of the electrolyte concentration. Curves 1, 2, 5, 6 (electrolytes 2:2), 3, 4, 7, 8 (electrolytes 2:1); curves 1–4 ($\xi = 1.03 \times 10^{14} s^{-1}$), 5–8 ($\xi = 0.52 \times 10^{14} s^{-1}$); curves 1, 3, 5, 7 ($\epsilon = 300k$), 2, 4, 6, 8 ($\epsilon = 150k$). ○: $CaCl_2$, ×: electrolyte 2:2[12], ⊗: Cl^-, ⊙: Na^+, △: K_2SO_4[22].

Table 1 Diffusion coefficients[20] for some ions at infinite dilution ($10^{-9} m^2 \times s^{-1}$).

Mg^{+2}	0.71
Ca^{+2}	0.79
Sr^{+2}	0.79
Zn^{+2}	0.72
NO_3^{-1}	1.92
IO_3^{-1}	1.09
IO_4^{-1}	1.45
SO_4^{-2}	1.08
CrO_4^{-2}	1.07

realistic charge distribution in the electronic clouds of the ions. As a consequence the self-diffusion coefficients are consistent with experimental data, mainly in the systems where the viscosity is the water viscosity ($\xi = 1.03 \cdot 10^{14} s^{-1}$), as seen in figure 1 and in Table 1.

The retention times of all groups of two ions found into a sphere centred on one of them were determined and recorded during the Brownian simulations of the systems. The resulting data form the frequency distribution function of the retention times, t_r, $P_{ij}(t_r, R_{ij})$, formally equalled to[1]:

$$P_{ij}(t_r, R_{ij}) = A(R_{ij})\, e^{-t_r/\tau(R_{ij})} + B(R_{ij})\, t_r^{-n(R_{ij})} + C(R_{ij})$$

or

$$P(t, R) = A(R)\, e^{-t/\tau(R)} + B(R)\, t^{-n(R)} + C(R) \qquad (7)$$

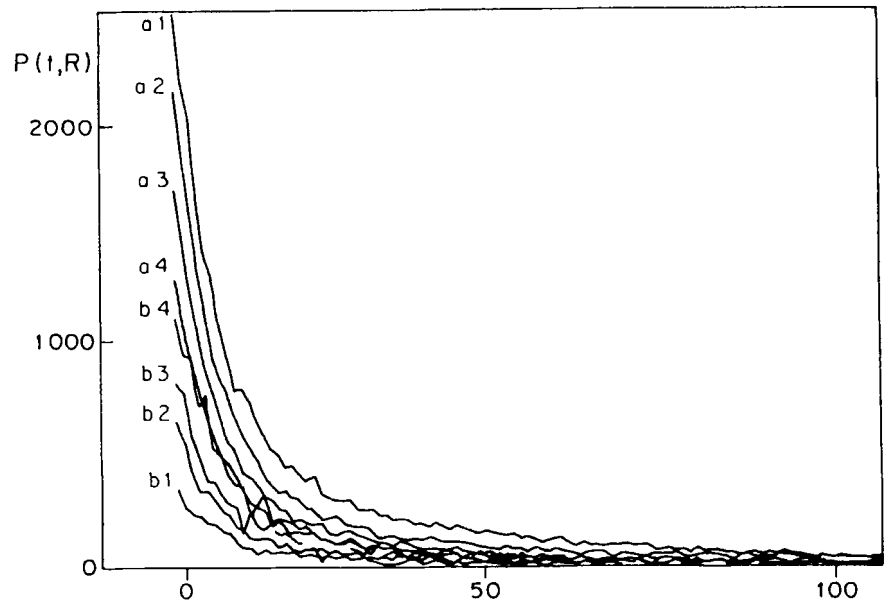

Figure 2 $P(t, R)$ as a function of the retention time ($10^{-14}s$), 2:2 electrolytes, $\xi = 0.52 \times 10^{14} s^{-1}$, $\epsilon = 150k$, C = 1.0 M. The limiting distances R are 1.05 for the curve (1), 1.15 (2), 1.25 (3) and 1.35σ (4); the lines *a* are *ij* pairs data and lines *b* are *ii* results.

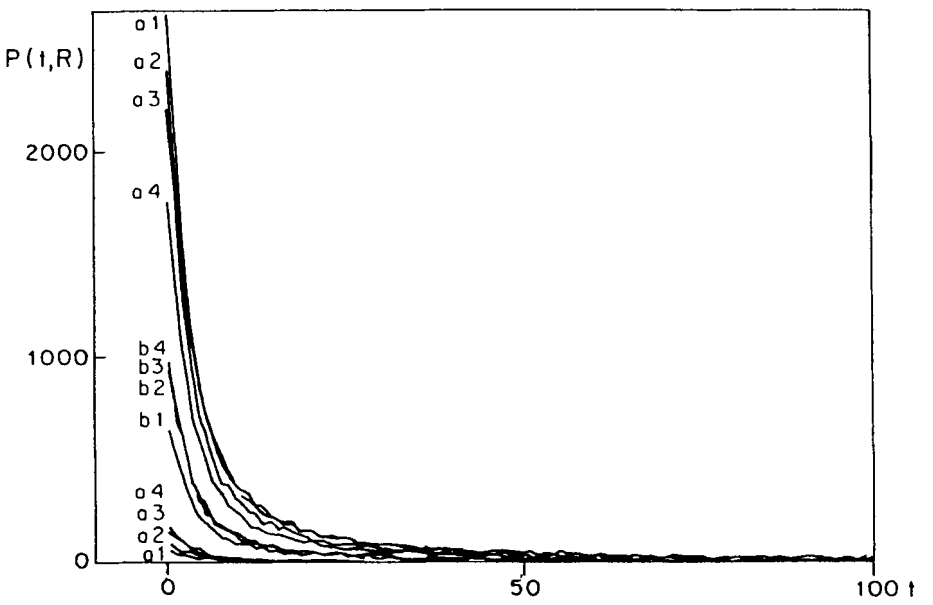

Figure 3 $P(t, R)$ as a function of the retention time ($10^{-14}s$), 2:1 electrolytes, $\xi = 1.03 \times 10^{14} s^{-1}$, $\epsilon = 300k$, C = 1.0 M. The limiting distances R are 1.05 for the curves (1), 1.15 (2), 1.25 (3); and 1.35σ (4); the lines *a* are anion-cation, *b* cation-cation and *c* anion-anion results.

where $A(R_{ij})$, $B(R_{ij})$, $C(R_{ij})$, $\tau(R_{ij})$ and $n(R_{ij})$ are functions to be determined. In the present paper, the values 1.05, 1.15, 1.25 and 1.35σ were used for $R_{ij} \equiv R$.

Figures 2 and 3 give some examples of the function $P(t, R)$ (all the figures show the complete set of data obtained on 100 000 time steps). In case the electrostatic energy is repulsive, the sequence of the probabilities is:

$$P(t, R = 1.05) < P(t, R = 1.15 < P(t, R = 1.25) < P(t, R = 1.35) \quad (8)$$

while the inverse sequence is correct for the repulsive electrostatic energy cases:

$$P(t, R = 1.05) > P(t, R = 1.15 > P(t, R = 1.25) > P(t, R = 1.35) \quad (9)$$

The $P(t, R)$ are not additive because of the dislocation in time resulting in changing the $P(t, R)$ sequencies according to the long range forces.

Each term of equation (7) presents its own behavior and meaning. The last rhs term, $C(R)$, is the limit for infinite distance of $P(t, R)$, so that we can write:

$$P_{ij}(t, \infty) = C_{ij}(\infty) = N_j \quad (10)$$

since all the ions of j kind (number N_j) are observed by the central i ion. Nevertheless the long time limit of $P(t, R)$ must be zero when $R < \infty$ since all the ions have a finite probability to leave the R shell in a finite time interval. As a consequence the long time behavior of $P(t, R)$ gives the relaxation to equilibrium:

$$N_{ij}(R) = \int_0^\infty P_{ij}(t, R)\, dt = \frac{4\pi}{3} R^3 \rho_j \quad (11)$$

where ρ_j is the bulk density for j species, so that $N_{ij}(R)$ is the mean number of j ions found in the neighbourhood of i ions in equilibrium conditions. This fact explains why very long retention times such as $10^{-10}\,s$ were observed in some cases while retention times greater than $4 \times 10^{-11}\,s$ are frequent in almost all experimental conditions. As a comparison, the kinetic theory mean collision time is about $5 \times 10^{-13}\,s$. The quantity $N_{ij}(R)$ is directly connected with the degree of binary association.

$\tau(R)$ must be interpreted as a relaxation time so that the first exponential term in rhs of equation (7) must described a collisional process. The $\tau(R)$ values are found to be independent of the concentrations [21] and of the R: their averages are given in Table 2.

The equations (4) and (7) represent the same property so that the three terms in equation (7) deduced from experimental evidences are to be related with the terms of equation (4). Since the correlation function of the velocities has a $t^{-d/d-1)}$ time dependence, the term $\exp(-t/\tau)$ must be interpreted as the decay process of loosing correlation between properties depending on the relative systematic forces.

Table 2 Mean values of $\tau(10^{-14}\,s)$.

Electrolyte:		2:2		2:1		
ϵ/k	$\xi(10\,s^{-1})$	ii	ij	$-2/-2$	$+1/+4$	$-2/+1$
150	0.52	3.4 (2)	3.4 (1)	3.3 (5)	3.6 (2)	3.5 (2);
300	0.52	3.3 (3)	3.3 (2)	3.6 (5)	3.7 (5)	3.6 (4)
150	1.03	2.1 (1)	2.03 (7)	2.1 (3)	2.0 (2)	1.92 (8)
300	1.03	2.04 (9)	2.00 (8)	2.1 (3)	2.0 (1)	2.0 (1)

So that as a first approximation:

$$H(t+t') = H(t')\, e^{-(t+t')/\tau} \tag{12}$$

The correlations between the relative systematic forces are then loosed because of the medium influence that acts by means of random collisions. This fact explains why this time decay does not depend on the interionic distance: this time decay is a solvent–solute process, not a solute–solute process. The temporal horizon is for the systematic forces a medium property not a property inherent to the solute. The decay of the correlations between the forces expressed by means of the relaxation time τ is faster in the more viscous media due to the more efficient brownian collisions.

The data for the A coefficients are plotted in Figures 4 to 11. In most of these cases, the A coefficients are functions quite linear of the concentration presenting also a strong energy dependence coherent with the interpretation of the loss of time correlations for properties depending upon the systematic forces. As can be seen in Figures 4 to 10, $A(\xi = 1.03 \times 10^{14} s^{-1}) > A(\xi = 0.52 \times 10^{14} s^{-1})$ so that the correlations of the forces are stronger when the medium is more viscous. On the contrary in equation (7), A is multiplied by the $\exp(-t/\tau)$ that presents a faster decay in the media with the highest viscosity. Anyway, the random forces tend to destroy the correlations between the forces: the net result favors the increase of the time to loose the relative systematic forces correlations together with the increase of the friction coefficient. The random forces destroy more easily the temporal correlations in attractive forces cases so that the A coefficients increase with R if the long range forces are repulsive and decrease if the forces are attractive. This effect together with the influence of the short range forces may superpose the curves for

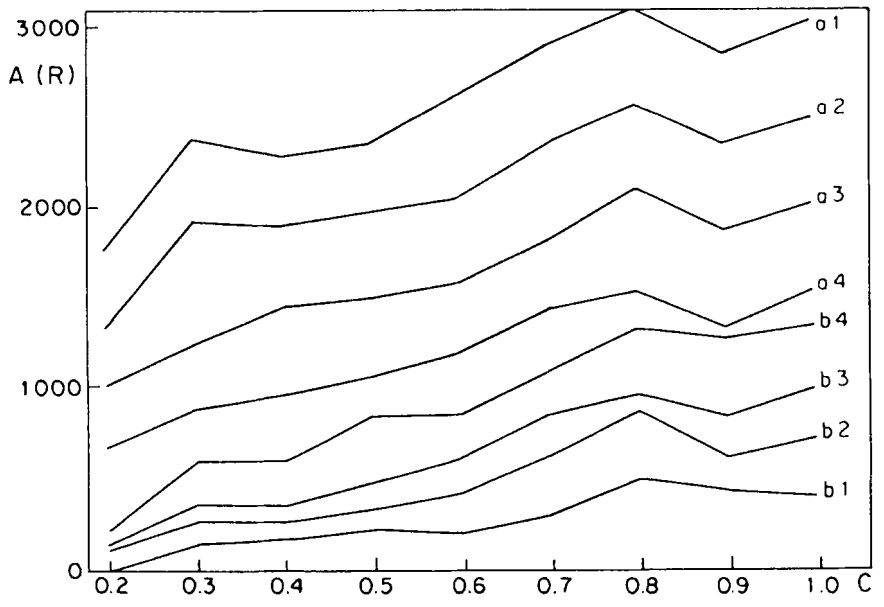

Figure 4 $A(R)$ as a function of the concentration ($mol \times l^{-1}$), 2:2 electrolytes, $\xi = 0.52 \times 10^{14} s^{-1}$, $\epsilon = 150k$, the curves as in Figure 2.

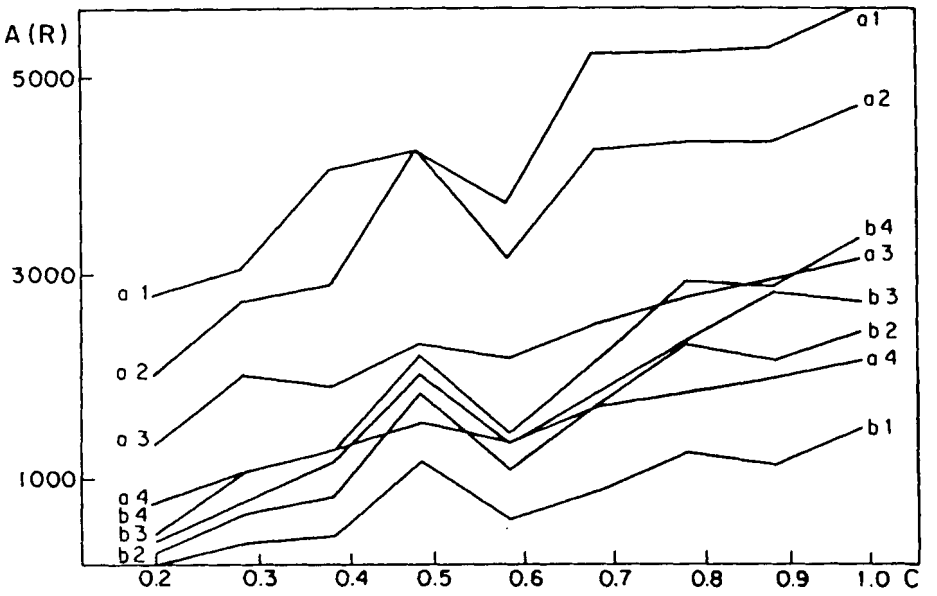

Figure 5 $A(R)$ as a function of the concentration ($mol \times l^{-1}$), 2:2 electrolytes, $\xi = 0.52 \times 10^{14} s^{-1}$, $\epsilon = 300k$, the curves as in Figure 2.

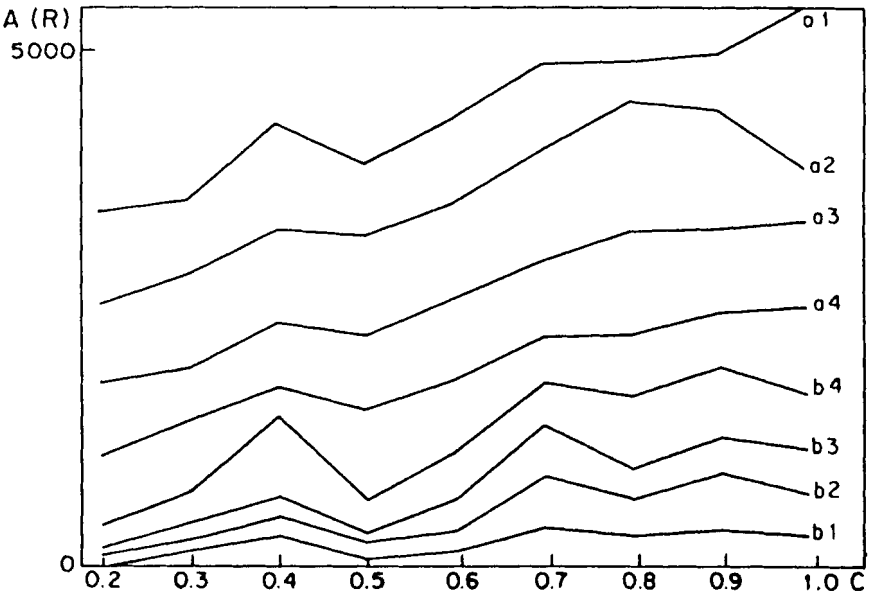

Figure 6 $A(R)$ as a function of the concentration ($mol \times l^{-1}$), 2:2 electrolytes, $\xi = 1.03 \times 10^{14} s^{-1}$, $\epsilon = 150k$, the curves as in Figure 2.

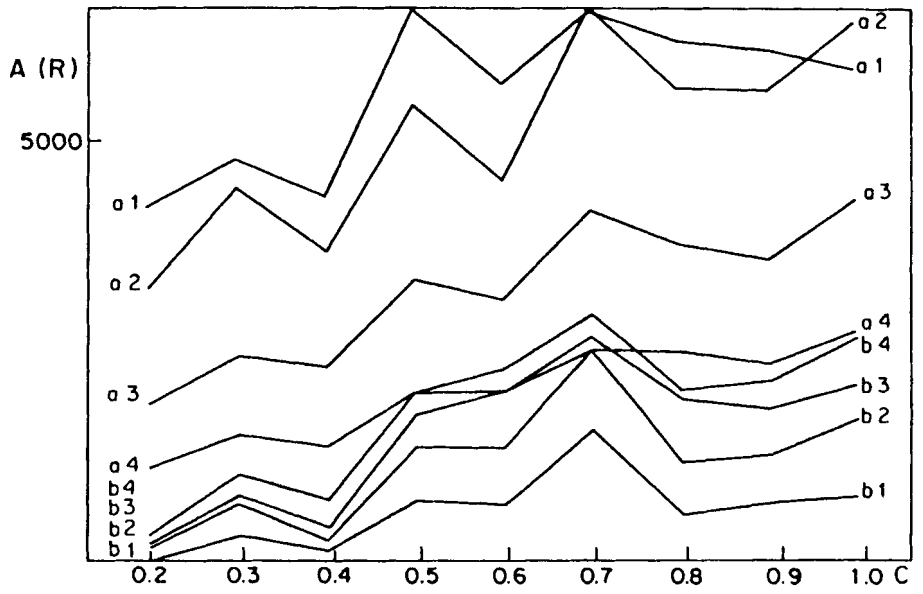

Figure 7 $A(R)$ as a function of the concentration ($mol \times l^{-1}$), 2:2 electrolytes, $\xi = 1.03 \times 10^{14} s^{-1}$, $\epsilon = 300k$, the curves as in Figure 2.

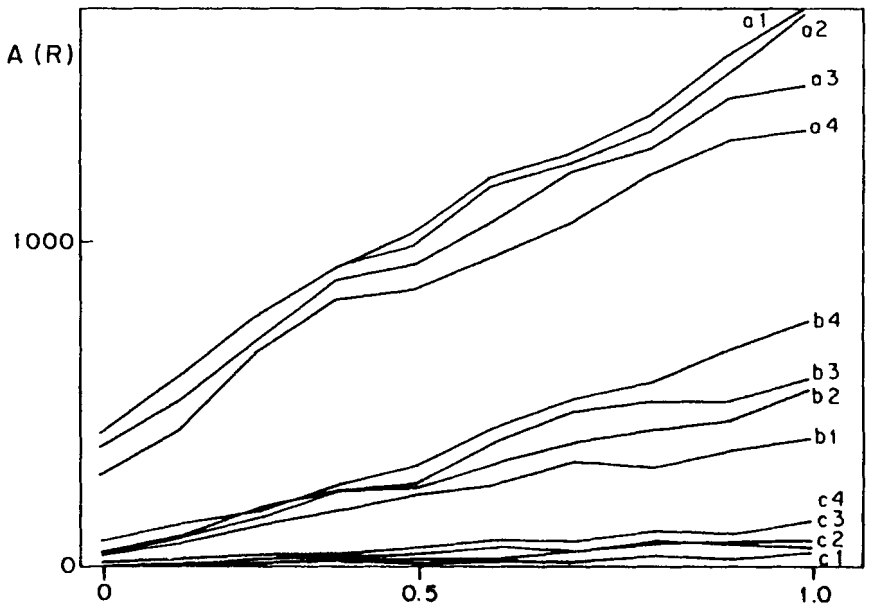

Figure 8 $A(R)$ as a function of the concentration ($mol \times l^{-1}$), 2:1 electrolytes, $\xi = 0.52 \times 10^{14} s^{-1}$, $\epsilon = 150k$, the curves as in Figure 3.

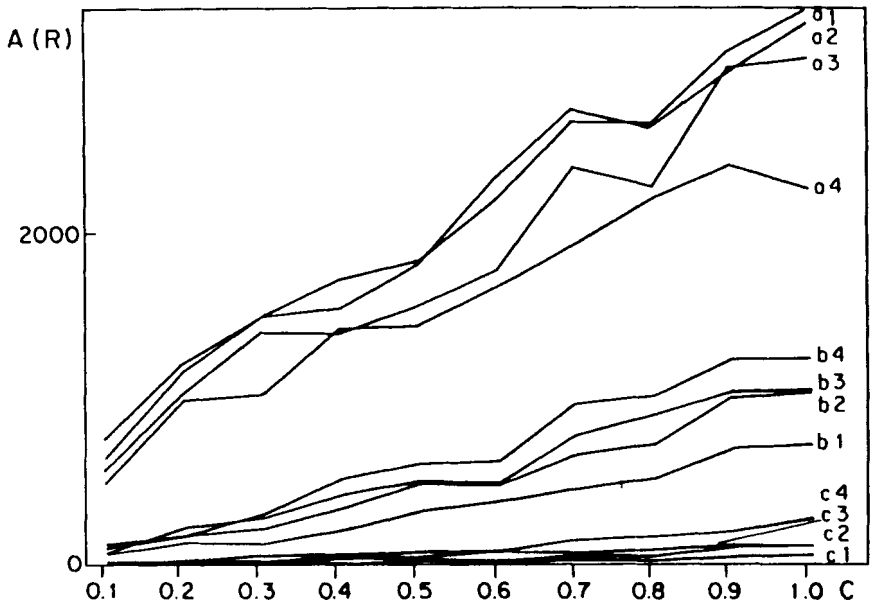

Figure 9 $A(R)$ as a function of the concentration ($mol \times l^{-1}$), 2:1 electrolytes, $\xi = 0.52 \times 10^{14} s^{-1}$, $\epsilon = 300k$, the curves as in Figure 3.

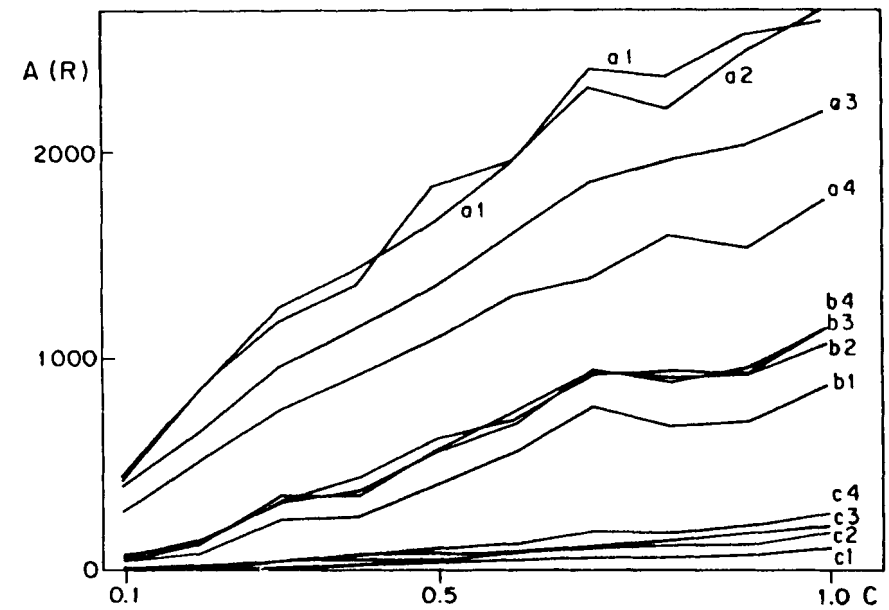

Figure 10 $A(R)$ as a function of the concentration ($mol \times l^{-1}$), 2:1 electrolytes, $\xi = 1.03 \times 10^{14} s^{-1}$, $\epsilon = 150k$, the curves as in Figure 3.

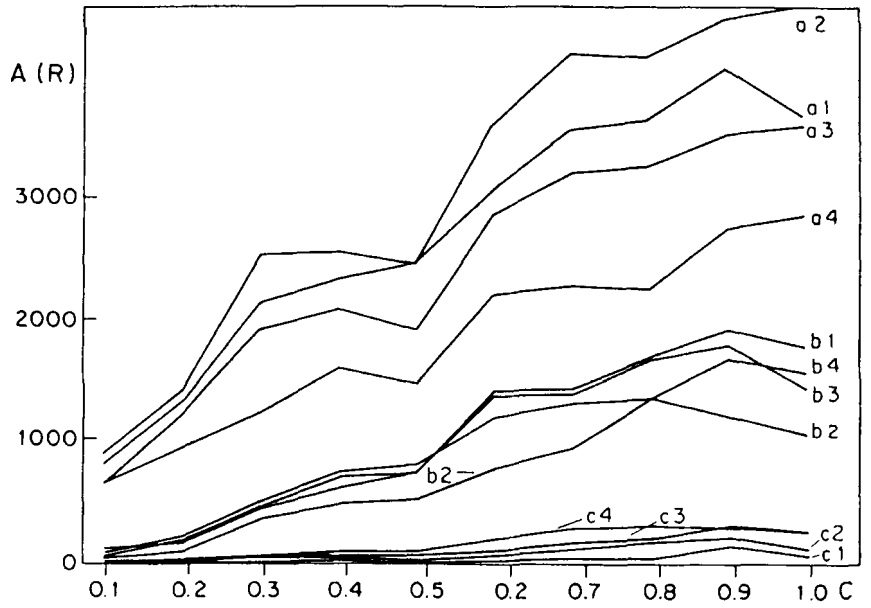

Figure 11 $A(R)$ as a function of the concentration ($mol \times l^{-1}$), 2:1 electrolytes, $\xi = 1.03 \times 10^{14} s^{-1}$, $\epsilon = 300k$, the curves as in Figure 3.

ions with opposite and equal electrostatic charges. In the cases of two opposite charged ions, $A(\epsilon = 300k) > A(\epsilon = 150k)$, $A(\xi = 1.03 \times 10^{14} s^{-1}) > A(\xi = 0.52 \times 10^{14} s^{-1})$. When the ionic charges are equal, the conclusion is identical relatively to the ξ dependence but a strong concentration dependence is observed when looking to the energies with opposite behavior at low and high concentration.

Such as τ, it was observed that n is also concentration independent. The resulting mean values are listed in Tables 3, 4 and 5. The average on all the experimental data is: $n = 1.46 \pm 0.18$. The resulting time dependence for $B \times t^{-n}$ is close to $t^{-d/(d-1)}$ or $t^{-3/2}$ suggesting that this kind of decay is similar to the long time decay of correlation functions ruled by hydrodynamic behavior. The $B(R)$ contribution in equation (7) is essentially hydrodynamic in nature and must be related to the correlation of the relative velocities given in equation (5). The B coefficients (equation 7) are concentration and R dependent (Figures 12–19). Their behaviors are not simple: the short R dependence is different from the longer R one

Table 3 Electrolyte 2:2: Mean values of n. The standard errors are about 0.5 for all data.

		ii pairs				*ij pairs*			
R/σ		1.05	1.15	1.25	1.35	1.05	1.15	1.25	1.35
ϵ/k	$\xi(10^{14} s^{-1})$								
150	0.52	1.42	1.49	1.58	1.56	1.52	1.48	1.51	1.53
150	1.03	1.53	1.54	1.45	1.50	1.48	1.44	1.56	1.42
300	0.52	1.42	1.50	1.47	1.42	1.50	1.40	1.50	1.46
300	1.03	1.49	1.46	1.44	1.43	1.48	1.38	1.44	1.40

Table 4 Electrolyte 2:1: Mean values of n for the anions–anions and cations-cations cases. The standard errors are about 0.5 for all data.

R/σ		1.05	1.15	1.25	1.35	1.05	1.15	1.25	1.35
ϵ/k	$\xi(10^{14}s^{-1})$								
150	0.52	1.50	1.54	1.43	1.55	1.46	1.46	1.55	1.50
150	1.03	1.44	1.45	1.44	1.38	1.49	1.55	1.55	1.45
300	0.52	1.46	1.42	1.47	1.37	1.40	1.40	1.38	1.38
300	1.03	1.40	1.34	1.32	1.39	1.41	1.37	1.32	1.33

Table 5 Electrolyte 2:1: Mean values of n for the anions–cations cases. The standard errors are about 0.5 for all data.

R/σ		1.05	1.15	1.25	1.35
ϵ/k	$\xi(10^{14}s^{-1})$				
150	0.52	1.54	1.43	1.52	1.49
150	1.03	1.40	1.55	1.45	1.52
300	0.52	1.48	1.41	1.52	1.40
300	1.03	1.29	1.20	1.38	1.42

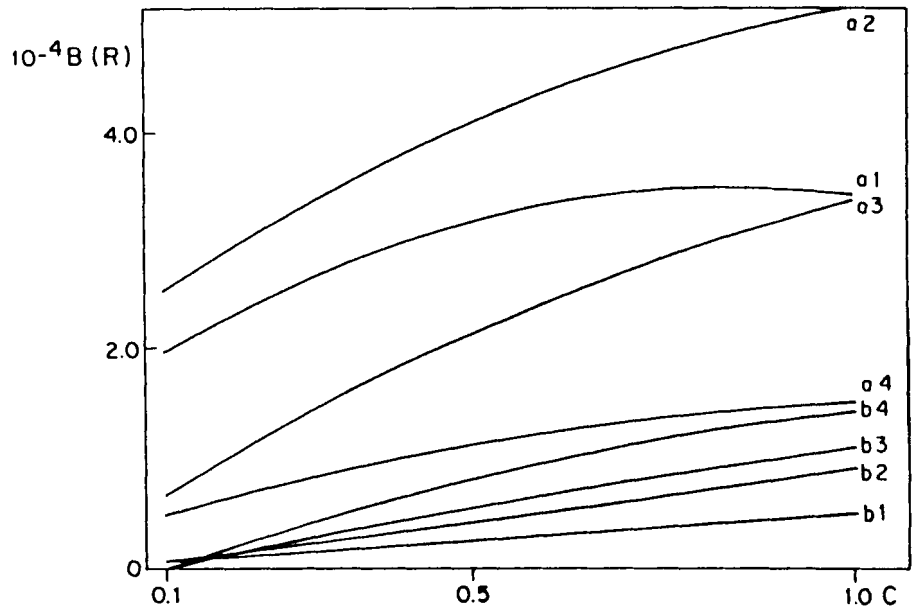

Figure 12 $B(R)$ as a function of the concentration ($mol \times l^{-1}$), 2:2 electrolytes, $\xi = 0.52 \times 10^{14} s^{-1}$, $\epsilon = 150k$, the curves as in Figure 2.

as can be seen on the Figures 20 and 21 presenting the averages of the $B(R)$ on all concentrations. The behavior in the inner shell ($R = 1.05\sigma$) must be considered as different from the behavior for $R = 1.15$, 1.25 and 1.35σ where a linear R dependence is observed. As a general feature, $B(R)$ increases with R when the energy is repulsive and decreases when the energy is attractive just as $A(R)$. A

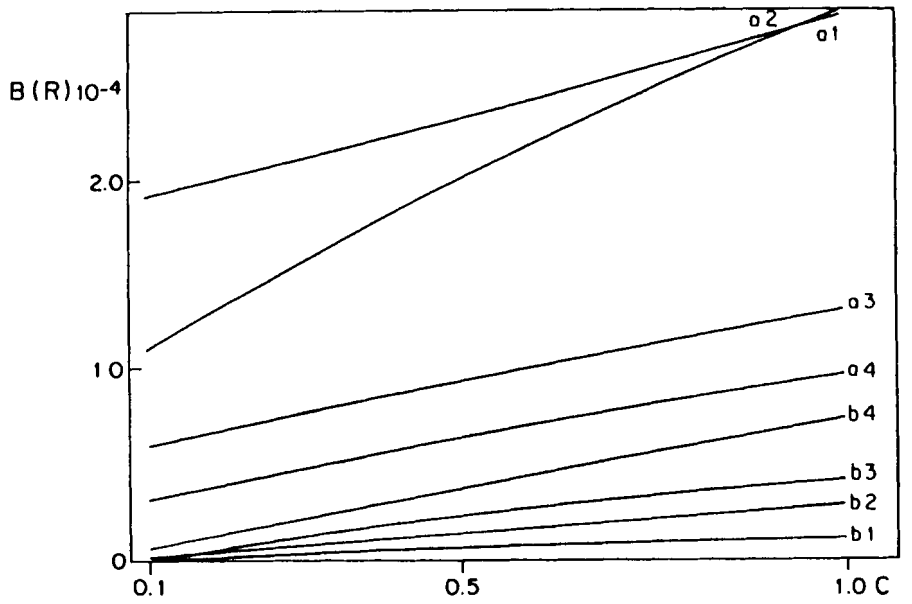

Figure 13 $B(R)$ as a function of the concentration ($mol \times l^{-1}$), 2:2 electrolytes, $\xi = 0.52 \times 10^{14} s^{-1}$, $\epsilon = 300\,k$, the curves as in Figure 2.

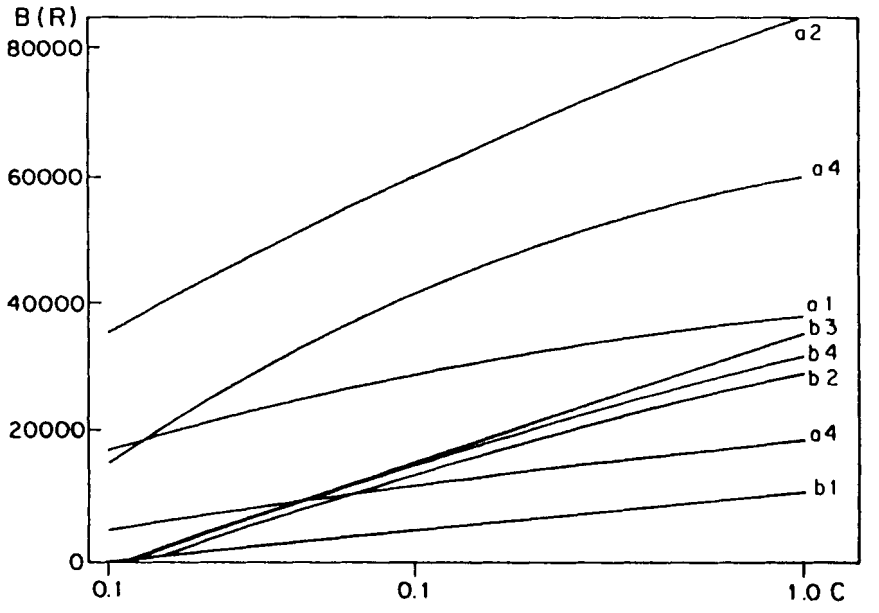

Figure 14 $B(R)$ as a function of the concentration ($mol \times l^{-1}$), 2:2 electrolytes, $\xi = 1.03 \times 10^{14} s^{-1}$, $\epsilon = 150\,k$, the curves as in Figure 2.

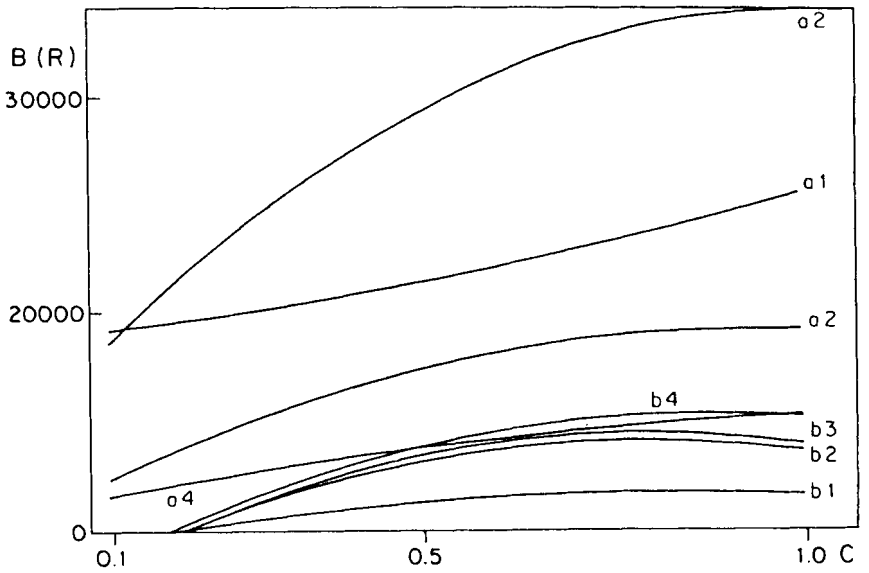

Figure 15 $B(R)$ as a function of the concentration $(mol \times l^{-1})$, 2:2 electrolytes, $\xi = 1.03 \times 10^{14} s^{-1}$, $\epsilon = 300\,k$, the curves as in Figure 2.

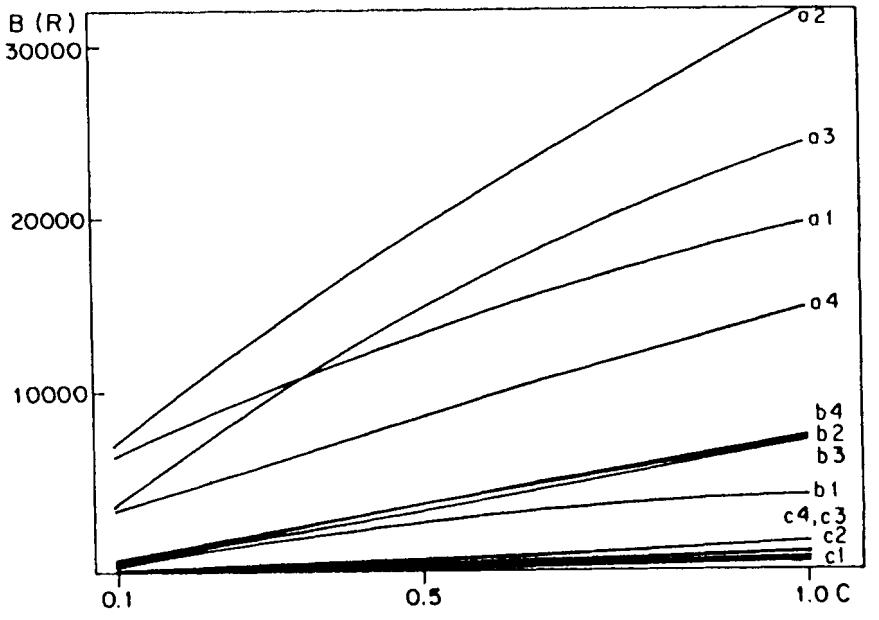

Figure 16 $B(R)$ as a function of the concentration $(mol \times l^{-1})$, 2:1 electrolytes, $\xi = 0.52 \times 10^{14} s^{-1}$, $\epsilon = 150\,k$, the curves as in Figure 3.

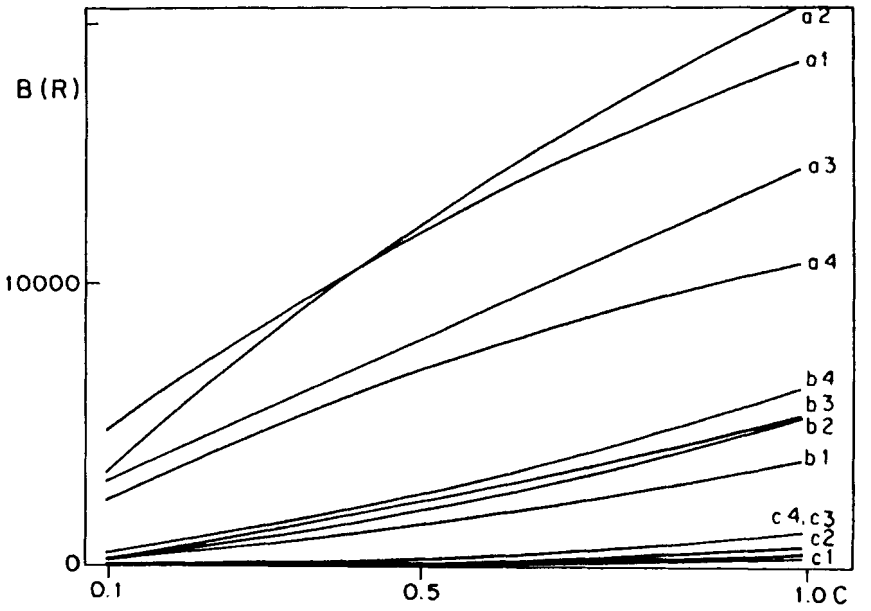

Figure 17 $B(R)$ as a function of the concentration ($mol \times l^{-1}$), 2:1 electrolytes, $\xi = 0.52 \times 10^{14} s^{-1}$, $\epsilon = 300k$, the curves as in Figure 3.

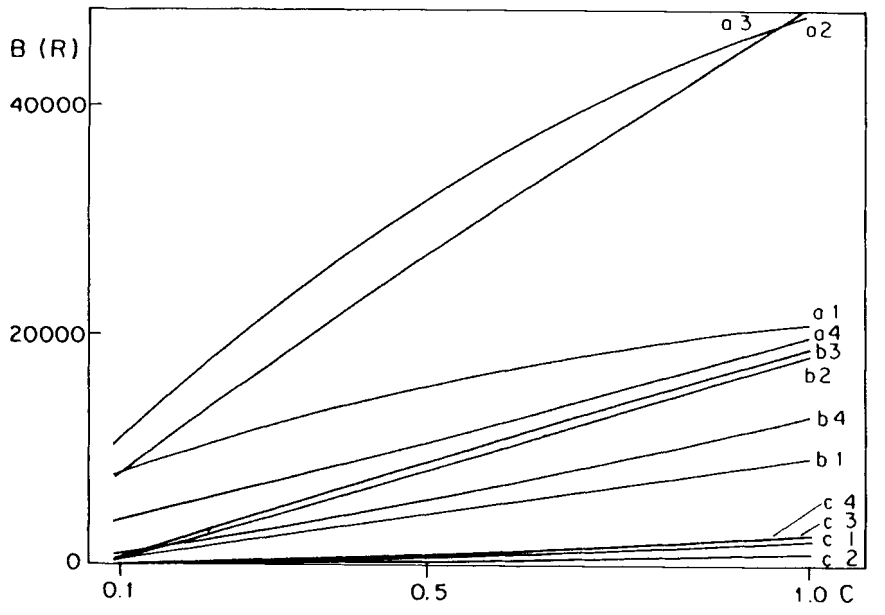

Figure 18 $B(R)$ as a function of the concentration ($mol \times l^{-1}$), 2:1 electrolytes, $\xi = 1.03 \times 10^{14} s^{-1}$, $\epsilon = 150k$, the curves as in Figure 3.

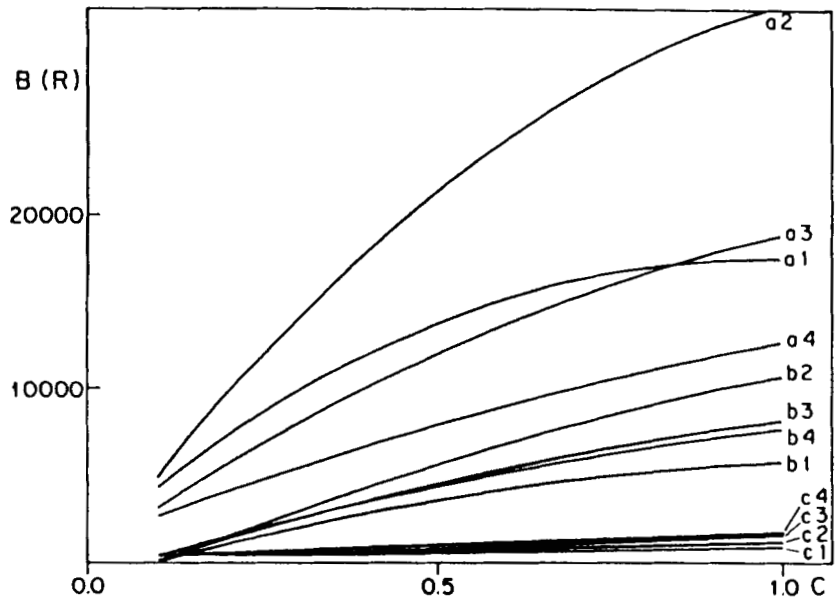

Figure 19 $B(R)$ as a function of the concentration ($mol \times l^{-1}$), 2:1 electrolytes, $\xi = 1.03 \times 10^{14} s^{-1}$, $\epsilon = 300k$, the curves as in Figure 3.

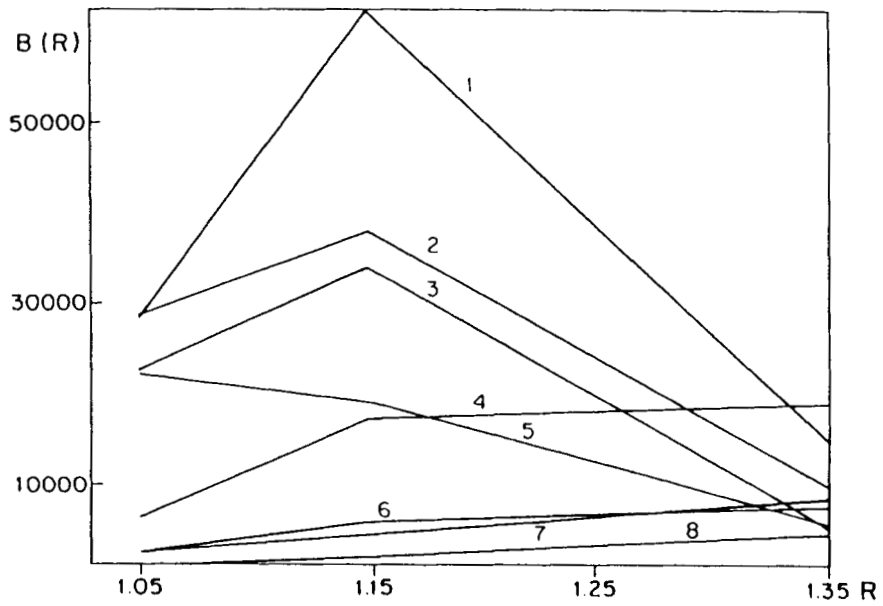

Figure 20 **Averages of the** $B(R)$ coefficients as function of R (σ), 2:2 electrolytes. The values for $\xi \times 10^{-14} \times s^{-1}$ and (ϵ/k) are 0.52, 300 for the lines 1 and 4; 0.52, 150 (2 and 7); 1.03, 300 (3 and 6) and 1.03, 150 (5 and 8). The curves 1, 2, 3 and 5 are *ij* data and the curves 4, 6, 7 and 8 are *ii* data.

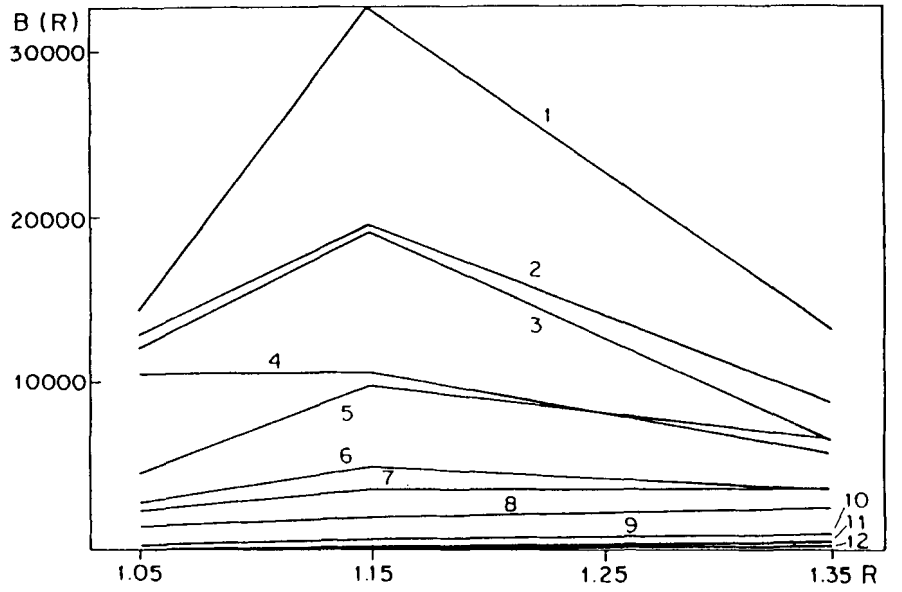

Figure 21 Averages of the $B(R)$ coefficients as function of R (σ), 2:1 electrolytes. The values for $\xi \times 10^{-14} \times s^{-1}$ and (ϵ/k) are 0.52, 300 for the lines 1, 5 and 9; 0.52, 150 (2, 7 and 11); 1.03, 300 (3, 6 and 10) and 1.03, 150 (4, 8 and 12). The curves 1 to 4 are anion-cation data, 5 to 8 cation-cation and the lines 9 to 12 are anion-anion data.

dependence on the friction coefficient can be also observed. The $B(R)$ concentration dependence is, in most cases, close to the linearity converging to a common value for the $B_{ij}(R = 1.15)$ at low concentration. The corrected ratios of the $B_{ij}(R = 1.15)$ coefficients are shown in Table 6 for some experimental conditions. The average of the ratios is 1.65 maybe suggesting also an exponent dependence in the dimensionality such as $[\xi/\epsilon]^{(d-1)/d}$ since $2^{2/3} = 1.587$. . . . The short R behaviors of $B(R)$ show meanwhile that they must depend on the interaction potential in a complex manner. The dependence on the long range forces can be seen in Table 7 where at high concentration (short Debye-Huckel length) the dependence looks like $|z_i z_j|^{(d-1)/d}$. At low concentration, the exponent increases

Table 6 Ratios $B_{ij}(\epsilon, \xi(10^{14} s^{-1}, R = 1.15\sigma)/B_{ij}(\epsilon', \xi', R = 1.15\sigma)$

	2:2, 1.0M	2:2, 0.2M	2:1, 1.0M	2:2, 0.1M
$\frac{B(150k, 0.52)}{B(300k, 0.52)}$	1.77	1.77	1.75	1.57
$\frac{B(150k, 1.03)}{B(300k, 1.03)}$	1.77	1.77	1.50	1.51
$\frac{B(150k, 1.03)}{B(150k, 0.52)}$	1.66	1.73	1.48	1.46
$\frac{B(300k, 1.03)}{B(300k, 0.52)}$	1.66	1.74	1.72	1.52

Table 7 Ratios of the $B_{ij}(2{:}2, 1.15\sigma)/B_{ij}(2{:}1, 1.15\sigma)$

ϵ	$\xi(10^{14}s^{-1})$	$C=0.2M$	$C=1.0M$
$150k$	0.52	2.85	1.58
$300k$	0.52	2.60	1.57
$150k$	1.03	2.56	1.77
$300k$	1.03	2.55	1.51

considerably: the energy dependence of $B(R)$ seems to be different considering either the short range either the long range forces.

CONCLUSIONS

The dynamical properties described by the correlation function $P(t, R)$ present two main features. The first is that the lifetime of two ions in an R shell is related to temporal correlations between their velocities: velocities which remain similar in direction and modulus allow a high retention time component in $P(t, R)$. The second main feature is that the net force, and its first derivative, acting on an ion remains correlated to the same properties of the another ion in R shell: long time correlations of the forces imply an high probability for a long time correlations between the velocities. The loss of the correlations occurs in a different manner for the velocity or the forces. The random component introduced in the velocity by the Brownian collisions is less than about 5% of the velocity at each time step during the dynamics simulation. As a consequence the loss of temporal information occurs slowly according to a $t^{-d/(d-1)}$ law.

The loss of the correlations on the relative forces is most critical because, as a liquid result, the random component of the force that is alone able to introduce a random component in the velocity of a few percents must be of the order of the total systematic force. The resulting time decay must therefore be very fast: the experimental results show that the correlation time $\tau \times \xi \simeq 1.7$–$2.1$. The dynamical behavior of the correlation between the forces presents two distinct aspects: the time decay is mainly dependent on the brownian collision while the initial probability (the A coefficient) for the presence of the ions in the R sphere depends mainly on the viscosity. All the components of the correlation function $P(t, R)$ depend upon the velocity or the systematic force directly or indirectly while the interionic distance remains less than R. This fact explains why the main features of the loss of the correlations must be associated either to the loss of the velocities correlations either to the loss of forces correlations.

The competition between the systematic forces, including in electrolyte solutions only attractive or attractive and repulsive components cannot be described in a simple way. Because of the profiles of the short and long range forces, direct consequences on the averages in equation (4) are observed. The correlations of the forces obey to a definite standard. In the case where the forces are attractive the correlations are maintained more efficiently at short distances while in the cases of predominantly repulsive forces, the correlations are lost very easily at short distance. The case of the correlations between the velocities for short R must be examined with a special care when the forces are mainly attractive. The standard is then broken down in this case: the strong acceleration at short interionic distances

is able to destroy the velocity correlation. This fact occurs up to the minimum of potential energy that is met for interionic distances from 1 to 1.05 σ according to the specific case. This conclusion implies that "the effect of the interionic pair potential would prevail over that of the concentrations"[12]. The amazing conclusion is that, regarding the relative interionic velocities, a strong interionic attractive energy does not favor the probability of presence at short distance unless a new energetic component is introduced in order to form a chemical bond.

Finally the connection with equilibrium properties can be analyzed by means of the pair association. The pair association is detected by the radial distribution function that is obtained as the probability distribution for the presence of ionic pair at the interionic distance r[1,4,7,8,13]. The radial distribution function is an equilibrium property with the meaning of an average over infinite time data. The detection of paired ions as an equilibrium property is in contradiction with the dynamical behavior: from a dynamical point of view, these pairs do not exist. The differences of interpretation is clear in reference 7 where the exponential decay at short time is interpreted as the decay of the number of ionic pairs. Nevertheless their real existence is not important for the models of electrolyte solutions. The experimental behavior of these solutions is coherent with a model of ions pairing that can be justified by the analysis of the dynamical behavior since pairs of ions with correlated dynamical properties present a net electrostatic charge that may be zero such as in the classical model. The last consequence is that the only particular interionic distance[1,11,21] that must be searched in order to definite the existence of associated ionic pairs is associated to the minimum of the potential energy (see Figure 20 and 21).

Acknowledgements

We are indebted to Drs. D. J. Henderson and M. Lozada-Cassou for the valuable discussions and the critical reading of the manuscript. We wish also to acknowledge and thank the Conselho Nacional de Desenvolvimento Cientifico e Tecnológico for the financial support.

SPECIAL APPENDIX

Some details of the simulation method that were not described in the text are: The systematic force is given by:

$$\mathbf{F}_{s,i}(t) = -\frac{\mathbf{r}}{\mathbf{r}} \times \frac{\delta[V_{Cou}(r) + V_{LJ}(r)]}{\delta r}$$

The simulations were initiated choosing the ions coordinates near the points of a face-centered cubic lattice. The initial velocities were sampled using the Maxwell-Boltzmann unidimensional velocity distribution for each cartesian coordinate. The data were registered only after the equilibrium phase that was identified by the reproductibility of the radial distribution functions. The reproductibility of the maximum of the first peak of $g_{ij}(r)$ within 1.5%. This fact was observed after 60,000, 160,000 or 260,000 integration steps. The temperature in the three space direction was maintained, at each step of the simulation, at 100 K. Fluctuations of the temperature in 2–3%.

During the simulations, the radial distribution functions were calculated as an

equilibrium criterion, the position and velocity correlation functions were also obtained for consistency and for testing the potential energy model against experimental data.

The retention distribution function were calculated identifying the ions distant by less than each R (1.05, 1.15, 1.25 and 1.35) and registering the retention times.

The $A(R)$, $B(r)$, $\tau(R)$ and $n(R)$ were obtained by regression using correlation coefficients in order to identified the parameters values.

References

[1] L. Degrève, "Degree of Binary Association in Electrolyte Solutions. The Roles of the Short-range Interionic Potential and of the Friction Coefficient", *J. Chem. Soc., Faraday Trans. 2*, **84,** 1645 (1988).

[2] P.J. Rossky, J.B. Dudowicz, B.L. Tembe and H.L. Friedman, "Ionic Association in Model 2-2 Electrolyte Solutions", *J. Chem. Phys.*, **73,** 3372 (1980).

[3] H.L. Friedman and B. Larsen, "Corresponding States for Ionic Fluids", *J. Chem. Phys.*, **70,** 92 (1979).

[4] W.H. Lee and R.J. Wheaton, "Conductance of Symmetrical, Unsymmetrical and Mixed Electrolytes. Part 2. Hydrodynamic Terms and Complete Conductance Equation", *J. Chem. Soc., Faraday Trans. 2*, **74,** 1456 (1978).

[5] G. Pastore, P.V. Giaquinta, J.S. Thakur and M.P. Tosi," Ionic Pairing in Binary Liquids of Charged Hard Spheres with Nonadditive Diameters", *J. Chem. Phys.*, **84,** 1827 (1986).

[6] N.J.B. Green, M.J. Pilling and P. Clifford, "Approximate Solution of the Debye-Smoluchowski Equation for Geminate Ion Recombination in Solvents of Low Permittivity", *Mol. Phys.*, **67,** 1085 (1989).

[7] J. Trullàs, A. Giró and J.A. Padró, "Langevin Dynamics study of NaCl Electrolyte Solutions at Different Concentrations", *J. Chem. Phys.*, **93,** 5177 (1990).

[8] F. Lantelme and P. Turq, "The Role of Coulomb Forces in the Properties of Ionic Liquids", *J. Chem. Phys.*, **81,** 5046 (1984).

[9] R.M. Fuoss, "Ionic Association. III. The Equilibrium between Ion Pairs and Free Ions", *J. Am. Chem. Soc.*, **80,** 5059 (1958).

[10] D.N. Card and J.P. Valleau, "Monte Carlo Study of the Thermodynamics of Electrolyte Solutions", *J. Chem. Phys.*, **52,** 6232 (1970).

[11] G.V. Ramanathan and A.L. Jensen, "Statistical Mechanics of Electrolytes and Polyelectrolytes. IV. A Theory of Higher Valence Electrolytes", *J. Chem. Phys.*, **84,** 3472 (1986).

[12] J.L.F. Abascal and P. Turq, "Cluster Structure in Model Electrolyte Solutions", *Chem. Phys.*, **153,** 79 (1991).

[13] P. Turq, F. Lantelme and D. Levesque, "Transport Properties and the Time Evolution of Electrolyte Solutions in the Brownian Dynamics Approximation", *Mol. Phys.*, **37,** 223 (1979).

[14] W.F. van Gunsteren and H.J.C. Berendsen, "Algorithms for Brownian Dynamics", *Mol. Phys.*, **45,** 637 (1982).

[15] S.A. Rogde and J. Hafskjold, "Equilibrium Properties of a 2:2 Electrolyte Model. Monte Carlo and Integral Equations Results for the Restricted Primitive Model", *Mol. Phys.*, **48,** 1241 (1983).

[16] P. Linse and H.C. Andersen, "Truncation of Coulombic Interactions in Computer Simulations of Liquids", *J. Chem. Phys.*, **85,** 3027 (1986).

[17] J.P. Valleau and L.K. Cohen, "Primitive Model Electrolytes. I. Grand Canonical Monte Carlo Computations", *J. Chem. Phys.*, **72,** 5935 (1980).

[18] S.G. Brush, H.L. Sahlin, E. Teller, "Monte Carlo Study of a One-component Plasma. I", *J. Chem. Phys.*, **45,** 2102 (1966).

[19] H. Van Beijeren, "Transport Properties from Stochastic Lorenz models", *Rev. Mod. Phys.*, **54,** 195 (1982).

[20] J. Heyrovsky and J. Kůta, *Principles of Polarography*, Publishing House of the Czechoslovak Academy of Sciences. Prague. Academic Press. New York (1965).

[21] M.C. Justice and J.C.Justice, "Ionic Interactions in Solutions. I. The Association Concepts and the McMillan-Mayer Theory", *J. Sol. Chem.*, **5,** 543 (1976).

[22] F.O. Raineri, M.D. Wood and H.L. Friedman, "Self-diffusion Coefficients of Ions in Electrolyte Solutions by Nonequilibrium Brownian Dynamics", *J. Chem. Phys.*, **92,** 649 (1990).